Phase transitions in flexible polymeric surfaces

Yacov Kantor* and David R. Nelson

Department of Physics, Harvard University, Cambridge, Massachusetts 02138

(Received 19 June 1987)

The statistical mechanics of polymerized surfaces with a finite bending rigidity κ' is studied via the Monte Carlo method. The model system consists of a hexagon, L atoms across, excised from a triangular lattice embedded in three-dimensional space. Nearest-neighbor atoms interact via an infinite-square-well potential, while the bending energy is proportional to the (negative) scalar product of unit normals to adjacent triangles. Self-avoiding interactions are not included. The largest hexagon considered ($L = 19$) consists of 271 atoms. Unlike linear polymers or liquid membranes, these surfaces undergo a remarkable finite-temperature crumpling transition, with a diverging specific heat. For small $\kappa = \kappa'/k_B T$, the surface is crumpled, and the radius of gyration R_g grows as $\sqrt{\ln L}$. For large κ we find that the surface remains flat, i.e., $R_g \sim L$. Our results demonstrate the presence of a finite-temperature (second-order) crumpling transition, and provide a lower bound on a related transition in real self-avoiding membranes.

I. INTRODUCTION

Recent theoretical investigations have explored the properties of flexible polymerized membranes.[1] Examples of such membranes are polymerized lipid monolayers or bilayers,[2] which are sufficiently cross-linked so as to have a nonzero in-plane shear modulus. Although the bending rigidity of lipid bilayers is often large, it may be possible to reduce the rigidity considerably by introducing short chain alcohol cosurfactants.[3] There are, moreover, reports of the synthesis and extraction of cross-linked poly(methyl methacrylate) from the surface of sodium montmorillonite clays.[4] The resulting polymers should be highly flexible, with properties similar to a two-dimensional (2D) gel. Both kinds of membranes can be modeled[1] by fixed-connectivity surfaces formed from a regular two-dimensional lattice of hard spheres embedded in three dimensions (3D); an infinite-square-well potential between the nearest neighbors constrains both the minimum and maximum distance between nearest-neighbor pairs of particles (hence, the name "tethered surfaces"). Tethered surfaces can be studied in much the same way as linear polymers. In particular, it has been shown that without self-avoidance, entropic effects cause the radius of gyration R_g to increase as $\sqrt{\ln L}$, where L is the linear size of uncrumpled surface. The introduction of self-avoidance leads to $R_g \sim L^\nu$, with[1] $\nu \approx \frac{4}{5}$.

Implicit in the above description is the idea of a surface which is crumpled on scales large compared to a finite persistence length $\xi(T)$. This is indeed the case in the model described above, where ξ is of order of a single interatomic distance.[1] This model included only central forces between atoms, but did not contain bending energy terms, with the expectation that introduction of such terms will not modify the asymptotic behavior. This expectation was based on an analogy with *linear* polymers and *liquid* membranes: For *linear* polymer

chains the persistence length determines an effective monomer size, and is always finite, with an Arrhenius temperature dependence.[5] Introducing bending or bending-and-twisting force constants along the chain only modifies the persistence length, with no effect on the asymptotic behavior.[6]

For membranes, the persistence length is basically a correlation length associated with order in the local normals to the surface.[7] It is believed that the persistence length is also finite in membranes with *liquidlike* in-plane order. It has been recently realized[8] that short-wavelength transverse oscillations (undulations) of liquid membranes reduce their effective rigidity on large length scales. Detailed renormalization group calculations of the bending rigidity[9] show that the persistence length of the surfaces diverges (exponentially) only at $T = 0$. As emphasized by Polyakov,[10] there is a useful analogy with two-dimensional models of Heisenberg ferromagnetism: the surface normals are like a (purely longitudinal) spin field, and a crumpled surface is like a Heisenberg paramagnet. The undulations which destroy long-range order in surface normals are similar to spin waves.

Recent investigations of the behavior of rigid membranes with the *fixed connectivity* of tethered surfaces reached a very different conclusion. It has been shown[11] that (at least in the limit of rigid membranes at low temperatures) the undulations of such surfaces interact via the in-plane elastic constants, in such a way that the effective rigidity *increases* on large length scales. This result immediately raises interesting questions regarding the relevance of the bending energy terms in polymerized membranes.

In this work we investigate the dependence of the asymptotic behavior of rigid membranes on their bending constant using Monte Carlo (MC) method. We show that these surfaces undergo a remarkable second-order phase transition from a crumpled (low rigidity, high temperature) phase, where the membranes essentially behave as the tethered surfaces described in Ref. 1, to a

flat phase where one can use the ideas of Ref. 11 to describe the deviations from a flat configuration. The simulations have been performed on hexagonal surfaces, up to $L = 19$ atoms across. Because of very large simulation times [in some cases, 50 days of CPU (central processing unit) time per data point on an Apollo DN460 computer] we could not include the excluded-volume interactions. Our conclusions, however, strongly suggest a related transition in real self-avoiding membranes as well. Some of our results have already been published.[12] Since then we have performed larger-length-scale simulations; this paper includes both the improved results and detailed information which has not been included previously.

In Sec. II we summarize the behavior of various kinds of random surfaces, and define the model system used in our simulations. When a tethered surface is constrained to lie in a plane, it behaves like an elastic solid, with entropic elastic constants, which are strictly proportional to the temperature T. In Sec. III we estimate the elastic constants of this 2D solid, which are needed as input into the theory of Ref. 11. In Sec. IV we describe the MC ("diffusive dynamics") method and estimate the relaxation times. In the Secs. V and VI we show that the surface indeed undergoes a phase transition: its asymptotic behavior changes from crumpled to flat, and the specific heat diverges near a second-order transition point. Sec. VII describes the correlations between the unit normals to the triangular faces of the surface. These normals are a natural candidate for an order parameter, and their behavior is qualitatively similar to the behavior of spins in *three*-dimensional Heisenberg ferromagnets. In Sec. VIII we argue that the crumpling temperature found here is actually a lower bound on a similar transition in real self-avoiding membranes. We suggest, however, that excluded volume interactions are a relevant perturbation at the actual phase transition, so that the critical exponents of self-avoiding surfaces are probably different. A brief discussion of the results, experimental tests, and possible future investigations is presented in Sec. IX.

II. MODEL SYSTEM

In this paper we consider a two-dimensional triangular array of atoms with positions $\{r_i\}$, embedded in three dimensions. The energy assigned to a particular configuration of particles is

$$\mathcal{E} = -\kappa' \sum_{\langle \alpha,\beta \rangle} (\mathbf{n}_\alpha \cdot \mathbf{n}_\beta - 1) + \sum_{\langle i,j \rangle} V(|\mathbf{r}_i - \mathbf{r}_j|) . \quad (2.1)$$

The first sum is over pairs $\langle \alpha,\beta \rangle$ of unit normals $\{\mathbf{n}_\alpha\}$ erected perpendicular to each elementary triangle in the surface (see Fig. 1). In methyl methacrylate polymer,[4] the "atoms" in Fig. 1 would represent nodes in the 2D cross-linked network. In a lipid membrane, the normals would be aligned along the long axes of the lipid molecules. The bending rigidity κ' plays the role of a "Heisenberg exchange coupling" between neighboring normals. The second summation in Eq. (2.1) is over neighboring pairs of atoms $\langle i,j \rangle$ in the array interacting via a tethering potential[1]
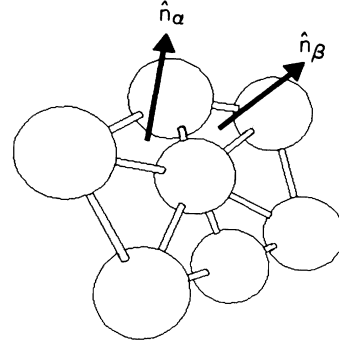

FIG. 1. A tethered surface: a hexagon of size $L = 3$ atoms across excised from a triangular lattice. Bonds indicate the pairs of atoms connected via square-well potential V. Spheres show the range of the repulsive (hard-core) part of potential V. Unit normals n, which are used to define bending energy, to two elementary triangles are shown.

$$V(r) = \begin{cases} 0 & \text{if } 1 < r < \sqrt{3} \\ \infty, & \text{otherwise.} \end{cases} \quad (2.2)$$

This potential consists of a hard-core repulsion (when the distance between the atoms becomes $r = 1$), and a part which causes neighboring atoms to behave as if tethered by a string, i.e., distance between them cannot exceed $r = \sqrt{3}$. The range of the repulsive (hard-core) part of potential V is represented by the size of the spheres in Fig. 1.

For $\kappa' = 0$, i.e., without the bending forces, this system has been extensively investigated.[1] It has been shown that at large-length scales it is described by a (continuum) free energy

$$\frac{\mathcal{F}_0}{k_B T} = \frac{1}{2} K \int d^2 x \left[\left[\frac{\partial \mathbf{r}}{\partial x_1} \right]^2 + \left[\frac{\partial \mathbf{r}}{\partial x_2} \right]^2 \right] , \quad (2.3)$$

where the discrete index of atoms has been replaced by a continuous 2D *internal* (i.e., attached to the surface) coordinate $\mathbf{x} = (x_1, x_2)$. This result is a consequence of crumpling of the surfaces, and the asymptotic form appears at length scales where the surface is already strongly crumpled.[1] Using the form (2.3) one can show[13,1] that the radius of gyration R_g of a surface L atoms across increases as $\sqrt{\ln L}$, i.e., it overfills the space (has an infinite fractal dimension). Not surprisingly, self-avoiding interactions play a very important role in crumpled tethered surfaces. Equation (2.3) can be used as a starting point in the investigation of surfaces with self-avoiding interactions.[1,14]

What happens when we combine bending rigidity with the fixed connectivity of a tethered surface? For small rigidity one might expect an increase in the persistence length, but no change in the asymptotic behavior. Investigations of the effects of rigidity usually take a point of view diametrally opposed to the crumpled surface ideas which underlie Eq. (2.3): One assumes that the surface is (at least locally) flat, and describes its fluctuations using the Monge parametrization in terms of a normal dis-

placement f, $\mathbf{r}(x_1, x_2) = (x_1, x_2, f(x_1, x_2))$. To lowest order in f and its gradients, the surface energy may be written[15]

$$\mathcal{F} = \tfrac{1}{2}\bar{\kappa} \int d^2x\, (\nabla^2 f)^2 + \tfrac{1}{2} \int d^2x\, (2\mu u_{ij}^2 + \lambda u_{kk}^2) \ , \quad (2.4)$$

where the strain matrix u_{ij} is related to f and the in-plane displacements u_i by $u_{ij} = \tfrac{1}{2}(\partial_i u_j + \partial_j u_i + \partial_i f \partial_j f)$, $\bar{\kappa}$ is the bending rigidity, and μ and λ are 2D Lamé constants. Using the Monge form of the normal,

$$\mathbf{n} = (\partial_1 f, \partial_2 f, 1)/(1 + |\nabla f|^2)^{1/2} \approx (\partial_1 f, \partial_2 f, 1) \ ,$$

it is straightforward to check that the first term in (2.1) reduces to the first term of Eq. (2.4) in the continuum limit, with $\bar{\kappa} = (2/3\sqrt{3})\kappa'$, plus boundary terms.

In the *liquid* membranes the second term of (2.4) vanishes, and, as discussed in the Introduction, this leads to a crumpled surface on sufficiently large length scales.[7-9] As discussed above, the surface also crumples when $\bar{\kappa}$ vanishes. When both terms in Eq. (2.4) are present simultaneously, however, nonlinear couplings between the undulations of the membrane are generated, and the transverse fluctuations are strongly suppressed.[11] The coupling between the modes is strong if the parameter

$$K_0 \equiv 4a^2\mu(\mu + \lambda)/(2\mu + \lambda) \ , \quad (2.5)$$

defined using the 2D Lamé constants and the lattice constant a, is much larger than $\bar{\kappa}$. In this limit one can show[11] that the effective bending constant depends on the size of the surface (measured in lattice constants) L as

$$\bar{\kappa}_{\mathrm{eff}} \approx L\sqrt{k_B T K_0} \ , \quad (2.6)$$

and that consequently the mean-square transverse fluctuations of the surface $\langle f^2 \rangle \sim L$. Unlike a crumpled surface the root-mean-square fluctuations normal to the surface are now small relative to the surface size. We can, therefore, expect that R_g of a tethered surface in this limit will be proportional to L. This also leads to long-range order in the normals to the surface, resembling the ordered phase of a Heisenberg ferromagnet. Since the treatment of Ref. 11 is valid only in the high-rigidity, low-temperature limit, it remains to be seen what happens as one reduces the rigidity or increases the temperature.

Clearly, the $\kappa' = 0$ and large-κ' results are not compatible, and one might expect a phase transition from a crumpled to flat phase as $\kappa = \kappa'/(k_B T)$ is varied. One must keep in mind, however, the possibility that the transition point may, in principle, occur at $\kappa' = 0$, meaning that any real surface is always asymptotically flat, or at $\kappa' = \infty$, meaning that the approximate treatment of Ref. 11 is not valid, and the bending energy is not relevant for large surfaces. Most of the effort of our simulations has been devoted to the proof that the transition appears at a finite value of the bending constant. We will show that the transition is continuous (second-order): the persistence length in the crumpled phase increases with increasing bending constant and diverges at a finite value of that constant; beyond that point the surface is asymptotically flat.

One should emphasize that (2.2) acts only between the neighboring atoms of the network. Our simulation did not include an excluded volume interaction between non-neighboring atoms, i.e., we are considering a *phantom* surfaces. As we shall see, these systems exhibit a low-temperature "flat" phase, where the neglect of self-avoidance is justified. We shall argue, moreover, that the finite-temperature crumpling transition discussed here for phantom surfaces is in fact a *lower bound* on a related transition in real self-avoiding membranes.

III. PROPERTIES OF PLANAR TETHERED SURFACES

In this section we describe the elastic properties of the membrane used in our simulation, when confined to a plane. With this constraint, the surface should behave like a two-dimensional isotropic solid with entropy-induced elastic constants.

The potential energy of the system in an allowed configuration is always zero, and the total energy will only include the trivial kinetic part of $\tfrac{1}{2}k_B T$ per degree of freedom, which will be the only contribution to the specific heat. The free energy per atom of such a two-dimensional solid has the form

$$\mathcal{F}_t = -\frac{k_B T}{N} \ln Z = k_B T \left[\ln \Lambda^2(T) - \frac{1}{N} \ln Q \right] \equiv \mathcal{F}_k + \mathcal{F}_c \ , \quad (3.1)$$

where Z is the partition function, $\Lambda(T)$ is the thermal de Broglie wavelength, N is the number of atoms, while the two terms in the brackets correspond to the kinetic and configurational parts of the free energy. The kinetic term $\mathcal{F}_k$ does not depend on the shape of the solid, while the configurational integral Q in $\mathcal{F}_c$ does not depend on the temperature. The elastic stiffness tensor $C_{ijkl} = \lambda \delta_{ij}\delta_{kl} + \mu(\delta_{ik}\delta_{jl} + \delta_{il}\delta_{jk})$ of an isotropic solid is given by the second derivative of the free energy with respect to the strain tensors η_{ij},[6]

$$C_{ijkl} = -\frac{k_B T}{\mathcal{A}} \frac{\partial^2 \ln Q}{\partial \eta_{ij}\, \partial \eta_{kl}} \ , \quad (3.2)$$

where $\mathcal{A}$ is the area ("volume") of the solid. Since Q does not depend on T, the elastic stiffness will be strictly proportional to T. The long-wavelength elastic properties should be similar to real polymerized amphiphiles, whose elasticity arises from a combination of van der Waals and covalent forces. The tethered solid will display, for example, long-wavelength phonons, whose frequency will depend on the temperature of the solid.

A simple, order-of-magnitude estimate of the elastic constants can be obtained by replacing the "square well" interaction (2.2) by a harmonic potential $V(r) = \tfrac{1}{2}kr^2$. Consider a pair of atoms confined to one dimension interacting via (2.2). The mean separation between the atoms and the variance of that separation will be ≈ 1.37 and 0.045, respectively, and will not depend on the temperature. Let us replace this binary system by a pair of atoms connected by a harmonic (Hookean) spring, and choose the length of the spring to be 1.37 and its force constant $k \approx 22k_B T$ to ensure the right size of the fluctuations. We now may replace the actual tethered solid

by a triangular lattice of harmonic springs of this strength. (Other simple replacements, obtained, e.g., by consideration of the pair of atoms in 2D, lead to very similar results.) The Lamé constants of the harmonic lattice are easily shown to be given by $\lambda = \mu = (\sqrt{3}/4)k$. From the above estimate of k we find that the Lamé constants are

$$\mu = \lambda \approx 10 k_B T . \tag{3.3}$$

The elastic constants can also be calculated directly from MC simulations of thermal fluctuations. It can be shown[16] that the elastic compliance tensor

$$S_{ijkl} = -\frac{\lambda}{4\mu(\mu + \lambda)}\delta_{ij}\delta_{kl} + \frac{1}{4\mu}(\delta_{ik}\delta_{jl} + \delta_{il}\delta_{jk}) \tag{3.4}$$

is related to the thermally induced strains $\{\eta_{ij}\}$ by

$$\mathcal{A}\langle \eta_{ij}\eta_{kl} \rangle = k_B T S_{ijkl} . \tag{3.5}$$

As in Ref. 1, we randomly chose an atom and attempted to move it by $s = 0.2$ in a randomly chosen direction. If the new position was permitted by the potentials (2.2), we updated the position of the atom; if it was forbidden, the atom was left in its original position. During a single "MC time unit," on the average, one attempt of position change is made for each atom. We excised an $L \times L$ parallelogram of a triangular lattice and equilibrated it in 2D. We started from a perfect triangular lattice configuration, performed the MC equilibration, and recorded the resulting configurations every $\tau_0 \equiv L^2/s^2$ MC time units, for the total time $t = 100\tau_0$. These times suffice to ensure both the statistical independence of configurations, and good averages.

To see that our 2D MC simulations are indeed equilibrated, note first that the motion of the surface is purely diffusive, so that its equations of motion can be schematically written as

$$\frac{k_B T}{\widetilde{\mathcal{D}}}\frac{\partial u}{\partial t} = c\nabla^2 u , \tag{3.6}$$

where u and c are a displacement and elastic modulus (here we suppress the detailed tensor notation), and $\widetilde{\mathcal{D}}$ is the diffusion constant of a unit surface area. The diffusion constant of a single atom is $4s^2$. Division of this result by the area per atom gives $\widetilde{\mathcal{D}} = 8s^2/(\sqrt{3}a^2)$, where a is the mean distance between the atoms. Solids governed by (3.6) will have spatially sinusoidal normal modes which decay exponentially in time with time constant dependent on the length scale of the oscillation. For a square solid of linear size La the lowest mode will have wavelength $2La$, and its relaxation time will be

$$\tau = \frac{L^2 k_B T a^4}{8\pi^2 s^2 c} . \tag{3.7}$$

Assuming that c is of order of few $k_B T$ (and $a \approx 1.34$) we find that $\tau \sim 0.1\tau_0$. This ensures that the time intervals between our measurements of the positions of the atoms were long enough to ensure statistically independent configurations.

To evaluate Eq. (3.5), one must associate a set of strains $\{\eta_{ij}\}$ with a given MC configuration. To do this,

we consider a succession of parallelograms built using two "basis vectors," $\mathbf{b}_1$ and $\mathbf{b}_2$, emerging from the same atom. As illustrated in Fig. 2, each of these vectors terminates in an atom n tethering units away. Their equilibrium length b is defined by the thermal averages $b^2 \equiv \langle (\mathbf{b}_1)^2 \rangle = \langle (\mathbf{b}_2)^2 \rangle$, while the angle between their mean directions is $\pi/3$, i.e., $\langle \mathbf{b}_1 \rangle \cdot \langle \mathbf{b}_2 \rangle = \frac{1}{2}b^2$. If at a particular moment these vectors have values $\mathbf{b}_1$ and $\mathbf{b}_2$, the instantaneous strain tensors within the parallelogram are

$$\eta_{11} = \frac{1}{2}\left[\frac{\mathbf{b}_1^2}{b^2} - 1\right] , \tag{3.8a}$$

$$\eta_{12} = \frac{1}{2\sqrt{3}l^2}(2\mathbf{b}_1^2 - \mathbf{b}_1 \cdot \mathbf{b}_2) , \tag{3.8b}$$

$$\eta_{22} = \frac{1}{6b^2}(4\mathbf{b}_2^2 + \mathbf{b}_1^2 - 4\mathbf{b}_1 \cdot \mathbf{b}_2) - \frac{1}{2} , \tag{3.8c}$$

where the x_1 axis has been chosen to coincide with the instantaneous direction of $\mathbf{b}_1$.

We considered the case of free boundaries, so that the elastic properties were measured at zero pressure. A typical equilibrium configuration is depicted in Fig. 2. A sequence of such configurations was analyzed to determine the thermal averages of strain-strain correlations, using the definition (3.8). (The averaging was performed over all configurations and over the possible positions of the origin of the basis vectors $\mathbf{b}_1$ and $\mathbf{b}_2$ in each configuration as well.) The length of the basis vectors (in lattice units) n ranged between 1 and $L - 1$. In a very large system $\langle \eta_{ij}\eta_{kl} \rangle$ eventually becomes proportional to n^2 (or to $\mathcal{A}$), and the compliance tensor (3.5) becomes independent of n. Therefore, we need to extrapolate our results to $1/n = 0$. On the other hand, our free boundary conditions are expected to lead to strong finite-size effects.

Figure 3 depicts three different components of S_{ijkl} as a function of $1/n$. The simulation has been performed
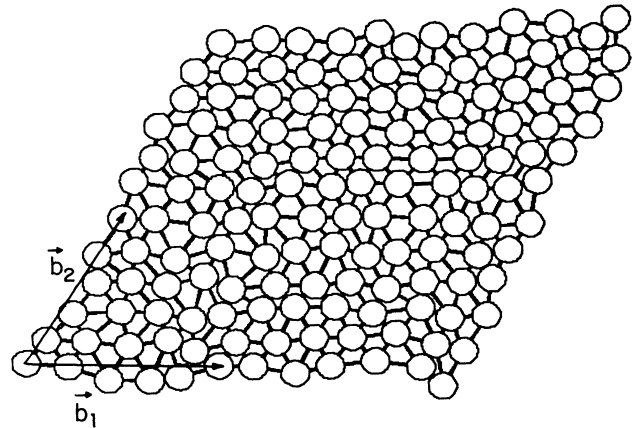

FIG. 2. Equilibrium configuration (at zero pressure) of a tethered solid in 2D (parallelogram of linear size $L = 12$ excised from a triangular lattice). Vectors $\mathbf{b}_1$ and $\mathbf{b}_2$ used to define strains are shown for the case $n = 5$.
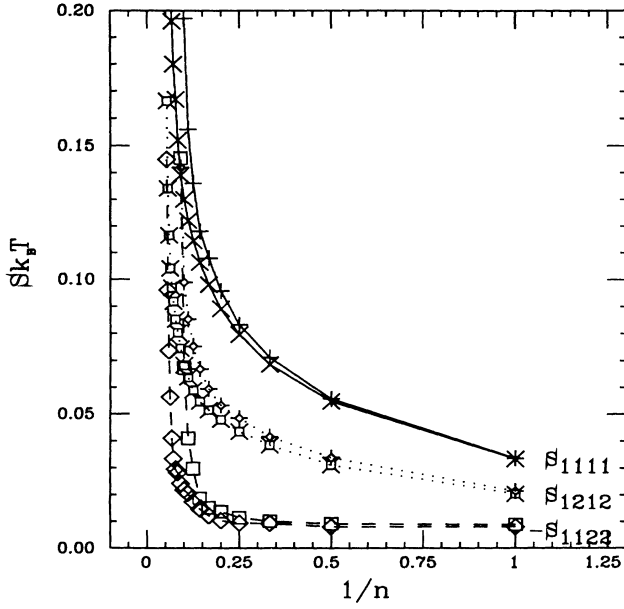
FIG. 3. Elements of the elastic compliance tensor S obtained from the strain fluctuations on the length scales of n lattice constants vs $1/n$. A pair of curves for each element of S corresponds to the results obtained from parallelograms with $L = 12$ (lower curve) and $L = 20$ (upper curve).

for $L = 12$ and $L = 20$. For $1 \leq n \leq 3$ we see a weak dependence of the compliance on $1/n$. However, for larger values of n, the compliance constants increase to very large values. One can clearly see that this is a finite size (boundary) effect by comparing the results of two different network sizes: for larger L, the sudden increase of the compliance is delayed to larger values of n. The importance of the finite size effects can also be seen by measuring the elastic constant S_{1112}, which is supposed to vanish in an isotropic solid. For $n \leq 3$ the calculated value of that constant is an order of magnitude smaller than S_{1111}, although for larger n, S_{1112} and S_{1111} gradually become comparable. Errors originating from statistical averaging can be estimated by comparing S_{1111} with S_{2222} which are calculated independently but should coincide. Differences between these two constants do not exceed a few percent, i.e., we got good averages. Results of Fig. 3 do *not* permit accurate extrapolation to the large-n limit. Our *estimate* of the extrapolated values (ignoring the finite size effects at large n) is

$$S_{1111} = (\lambda + 2\mu)/[4\mu(\lambda + \mu)] \approx 0.085/(k_B T) \ ,$$

$$S_{1122} = -\lambda/[4\mu(\lambda + \mu)] \approx -0.01/(k_B T) \ ,$$

and

$$S_{1212} = 1/(4\mu) \approx 0.045/(k_B T) \ .$$

These *three* estimates are supposed to produce *two* Lamé constants λ and μ. They are in fact approximately consistent giving

$$\mu \approx 5.4 k_B T \ , \tag{3.9a}$$

$$\lambda \approx 1.4 k_B T \ , \tag{3.9b}$$

results which should be contrasted with the rough estimate (3.3).

In Ref. 11 it is shown that the renormalized wave-vector-dependent rigidity $\tilde{\kappa}_R$ is renormalized by elasticity to lowest order in perturbation theory as follows:

$$\tilde{\kappa}_R(q) = \tilde{\kappa} + \frac{K_0 k_B T}{a^2} \int \frac{d^2 k}{(2\pi)^2} \frac{|\hat{q}_i P_{ij}(\mathbf{k})\hat{q}_j|^2}{\tilde{\kappa}|\mathbf{k} + \mathbf{q}|^4} + \cdots \ , \tag{3.10}$$

where $P_{ij}(\mathbf{k}) = \delta_{ij} - k_i k_j / k^2$ is the transverse projection operator. Taking the limit $q \to 0$ and restricting the wave-vector integration to $k > \pi/(La)$ we find that the second term exceeds the first when $L > L_c$, where

$$L_c \approx \left[\frac{32\pi^3 \tilde{\kappa}^2}{3 k_B T K_0} \right]^{1/2} \ . \tag{3.11}$$

Here, L_c is measured in lattice constants, and K_0 is given by Eq. (2.5). From the measured values of μ, λ, and a in a simulation of a tethered surface confined to a plane, we find that $K_0 \approx 22 k_B T$, so that nonlinearities should have a strong effect on the bending undulations characteristic of a purely liquid membrane, whenever $L \gtrsim 4\tilde{\kappa}/k_B T \approx 1.5\kappa'/(k_B T) = 1.5\kappa$. We conclude that the surface studied here will be dominated by elastic effects at quite modest values of L over a wide range of κ values.

IV. MONTE CARLO PROCEDURE AND RELAXATION TIMES

We now allow the membrane to bend out of the plane, and use the MC method to investigate the spatial conformations and thermodynamic properties of surfaces with bending energy in three dimensions. We used the Hamiltonian (2.1) with nearest-neighbor potential (2.2). The procedure resembles the one explained in Sec. III. The random moves by amount $s = 0.2$ are made in 3D. The move is always accepted if the energy of resulting configuration E_f does not exceed the original energy E_i. If $E_i < E_f$, the move is accepted with probability $\exp[(E_i - E_f)/k_B T]$. The outcome of this equilibration procedure depends only on one parameter, the dimensionless rigidity $\kappa \equiv \kappa'/k_B T$. Our simulations were carried out on a hexagon with diameter of L atoms ($L = 3, 5, 7, 11, 15, 19$). When an atom is moved the bending energy embodied in (2.1) makes $E_f - E_i$ depend on the 3D positions of six nearest neighbors and six next nearest neighbors as well. This, together with long equilibration times, creates quite a time consuming procedure: the largest ($L = 19$) hexagon required 50 days of CPU time on an Apollo DN460 computer for each value of κ. For this reason we did not attempt to include the repulsive (excluded volume) interactions between the atoms which were not nearest neighbors on the triangular network.

In Fig. 4 we depict equilibrium configurations of the surface for several values of κ. We observe a dramatic change in the shape of surface. As will be shown in the
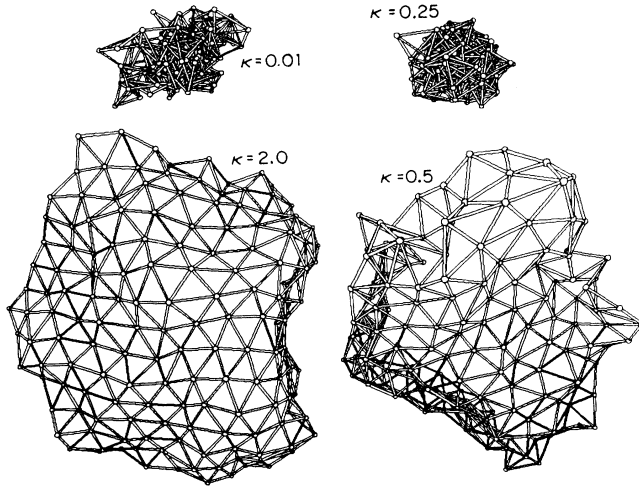
FIG. 4. Equilibrium configurations of hexagons with $L=15$ in the crumpled phase ($\kappa=0.01$ and 0.25), in flat phase ($\kappa=2.0$), and in semicrumpled region ($\kappa=0.5$) closer to κ_c.

FIG. 5. Time dependence of the squared radius of gyration R_g^2 (with $L=11$) for several values of κ, indicated near the curves. In the crumpled phase ($\kappa<\kappa_c$) both R_g^2 and its fluctuations increase with increasing κ. In the flat phase ($\kappa>\kappa_c$) R_g^2 increases and its fluctuations decrease with increasing κ, towards the values typical of a 2D tethered solid.

following sections the surface undergoes a second-order phase transition from a "crumpled" to "flat" state. Not surprisingly, for small values of κ, the surface has the same qualitative behavior as in the case of $\kappa=0$, which has been investigated in the previous publications.[1] In this regime the surface overfills the space (has an infinite fractal dimension). In this simulation we measured strongly fluctuating quantities, whose rms fluctuations were of order of the quantities themselves. Quantitative measurement of such properties requires the total simulation time to exceed the relaxation times by a significant factor, to ensure a reasonable accuracy of the average.

For $\kappa=0$, the relaxation time (or the time between two statistically independent configurations) is given by[1] the Rouse relaxation time $\tau_R \approx \tau_0 = N/s^2$, where $N=(3L^2+1)/4$ is the number of atoms in the surface. The total simulation time for each κ was $300\tau_0$ for $L\leq 11$, $500\tau_0$ for $L=15$, and $1000\tau_0$ for $L=19$. Such simulation times produce good statistical averages for small κ.

In Fig. 5 we show the time dependence of the radius of gyration of the surfaces for several values of κ with $L=11$. Notice that for small κ's both R_g^2 and its fluctuations increase with increasing κ. For larger κ's this tendency disappears: the surface becomes flat and the changes in R_g^2 are essentially governed by the fluctuations of the in-plane size of the 2D tethered solid described in Sec. III.

Although the Rouse relaxation time controls the dynamics for small κ, a different dynamical mechanism controls the relaxation when the membrane is flat. In the limit of large κ the relaxation times of the surface are determined by the transverse fluctuations (undulations) of the surface. (The in-plane relaxation times, which have been discussed in Sec. III, are significantly shorter than the times required by the transverse motions.) If we disregard the in-plane interactions between different undulations, the equation of motion follows directly from the first term in (2.4)
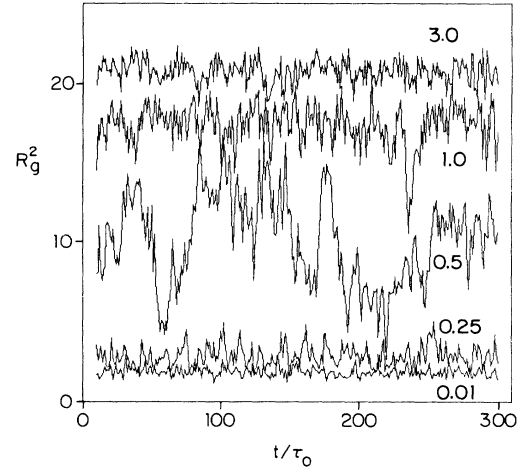
$$\frac{\partial f}{\partial t}=B(\nabla^2)^2 f \ , \tag{4.1}$$

with $B=\bar{\kappa}m$, where m is the mobility (ratio between the applied force and the drift velocity) of a unit surface area. In our MC procedure the mobility of a single atom is $s^2/(12k_BT)$, and therefore $m=s^2a^2\sqrt{3}/(24k_BT)$, where a is the lattice constant of the 2D tethered solid. Thus

$$B=s^2a^2\bar{\kappa}/(8\sqrt{3}k_BT)=s^2a^2\kappa/36 \ .$$

The eigenmodes of (4.1) will decay exponentially in time, $f(t,x)=f_0(x)e^{-t/\tau_f}$, and the decay times τ_f will be determined from the solution of an eigenvalue problem $B(\nabla^2)^2f_0(x)=-f_0(x)/\tau_f$. This is a well-known problem of vibrations of thin plates.[15]

We are not aware of a solution of plate with hexagonal geometry, so we use a square plate geometry to estimate τ_f. The slowest eigenmode in a square plate of linear size $\mathcal{L}$ with free boundaries satisfies[15]

$$\frac{\mathcal{L}^2}{\sqrt{B\tau_f}}=22.4 \ . \tag{4.2}$$

We expect the corresponding eigenmode of a hexagon to be located between the eigenmodes of inscribed and circumscribed squares. We shall therefore approximate our system by a square of linear dimensions $\mathcal{L}=\beta La$, with $\beta=0.7\pm0.3$, where the lower and upper limits correspond (approximately) to the cases of maximal inscribed and minimal circumscribed squares, respectively. Thus the relaxation time is given by

$$\tau_f=\frac{36\beta^4L^4a^2}{22.4^2s^2\kappa}\approx\frac{0.26\beta^4N\tau_0}{\kappa}\approx0.05\frac{N\tau_0}{\kappa} \ . \tag{4.3}$$

For, say, $L=19$ (with $\kappa\sim 1$) the simulation time is 2 or-

ders of magnitude larger than τ_f, and we expect to have a well-equilibrated system, while the averages will be accurate up to a few percent.

The above estimates of relaxation times may not be valid close to the transition point, where one expects critical slowing down. Direct measurement of the auto-correlation function indicates that the simulation time is still much larger than the relaxation times, so we may expect to have reasonable statistical averages.

V. SIZE AND SHAPE OF POLYMERIZED MEMBRANES

To quantify the nature of the crumpled and flat behaviors depicted in Fig. 4 and to establish the validity of the claim that these apparently different behaviors indeed reflect two different asymptotic regimes, we measured several shape parameters of the surface for various values of L and $\kappa = \kappa'/k_B T$. In particular we measured the radius of gyration of the surface

$$R_g^2(L,\kappa) \equiv \frac{1}{2N^2} \sum_i \sum_j \langle \, | \mathbf{r}_i - \mathbf{r}_j |^2 \, \rangle \, , \qquad (5.1)$$

where $N = (3L^2 + 1)/4$, and $\langle \, \rangle$ denotes the average over the configurations. For $L \leq 15$ we scanned the entire range of κ's, while for $L = 19$ we concentrated on the values close to the anticipated transition point. This information is summarized in Fig. 6. The steep increase of R_g of large surfaces at $\kappa \sim 0.3 - 0.4$ indicates the presence of the transition. We shall demonstrate a qualitative difference between the large-L behavior of R_g of the surfaces as a function of their linear size at the two sides of the transition point
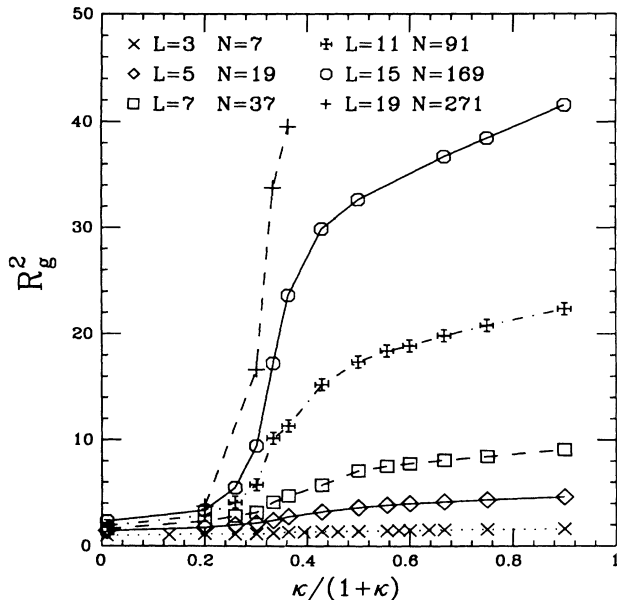
$$R_g(L) \underset{L \to \infty}{=} \begin{cases} \xi \sqrt{\ln L} & \text{for } \kappa < \kappa_c \\ \zeta L & \text{for } \kappa > \kappa_c \, . \end{cases} \qquad (5.2)$$

The parameter ξ measures the persistence length of a surface which has the same qualitative behavior as the *phantom* surfaces with $\kappa = 0$, which have been investigated in Ref. 1. The high-κ (low-temperature) part of (5.2) represents the behavior in the expected flat regime, where the coefficient ζ measures the possible shrinkage of a macroscopically flat surface due to small-length-scale fluctuations. Both ξ and ζ depend on κ, i.e., on the temperature.

Equation (5.2) represents only the asymptotic behavior of R_g, as $L \to \infty$. For small L we may expect the effective values of ξ and ζ to depend on L. We can *define* the effective values of the parameters via $\xi(\kappa, 1/L) \equiv R_g/\sqrt{\ln L}$ and $\zeta(\kappa, 1/L) \equiv R_g/L$, and attempt an extrapolation to $1/L = 0$. Figure 7 depicts the L dependence of the inverse persistence length. We expect the transition from crumpled to flat regime to occur via the divergence of ξ near the transition point. Indeed, for small κ the curves extrapolate to a constant as $L \to \infty$, while for large κ the $1/\xi$ decays to zero. Figure 8 depicts the effective values of ζ. For large κ these values tend to a constant as $L \to \infty$. For small κ they decay to zero. The extrapolated values of ξ and ζ can be obtained by assuming that both $1/\xi$ and ζ approach their asymptotic values as $A_1 + A_2/L$. Fitting to this form presumes that finite-size effects are controlled by atoms near the boundary. Within the limited accuracy of our measurement the extrapolated values are not very sensitive to the method of extrapolation. Figure 9 summarizes the extrapolated values of the parameters. No-
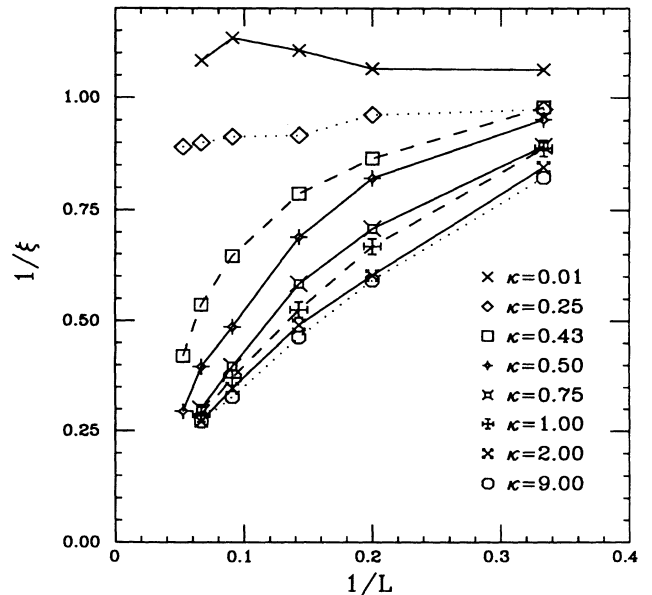

FIG. 6. Squared radius of gyration R_g^2 as a function of κ for several values of surface size L.

FIG. 7. Effective values of inverse persistence length $1/\xi$ (see text) vs $1/L$. For small κ persistence length extrapolates to a finite value in the limit $1/L = 0$. For large κ the quantity $1/\xi$ appears to vanish in this limit.
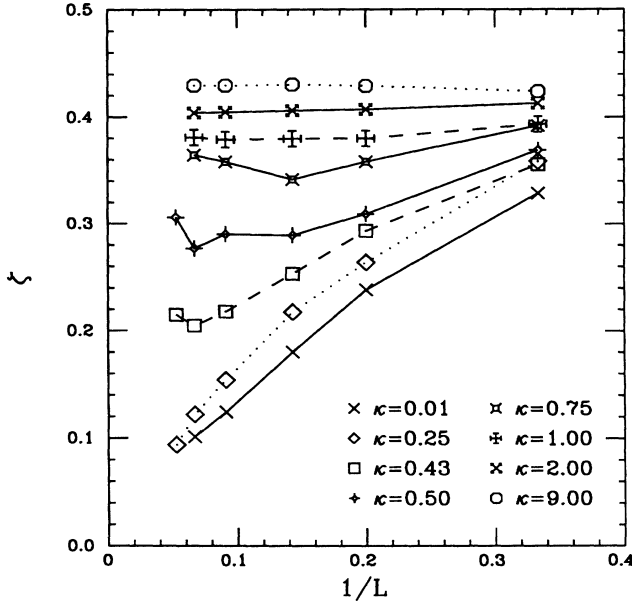
FIG. 8. Effective values of ζ (see text) vs $1/L$. For large κ the parameter ζ extrapolates to a finite value in the limit $1/L=0$. For small κ it apparently decays to zero in that limit.

tice, that the divergence of ξ and vanishing of ζ appears in the same narrow region of values of κ. From this figure we estimate $\kappa_c = 0.33^{+0.07}_{-0.03}$ and hypothesize a continuous-phase transition as $L \rightarrow \infty$.

Precisely at the transition, one might expect intermediate "semicrumpled" behavior, i.e.,

$$R_g \approx aL^{v'} , \tag{5.3}$$

where a is the mean distance between two neighboring
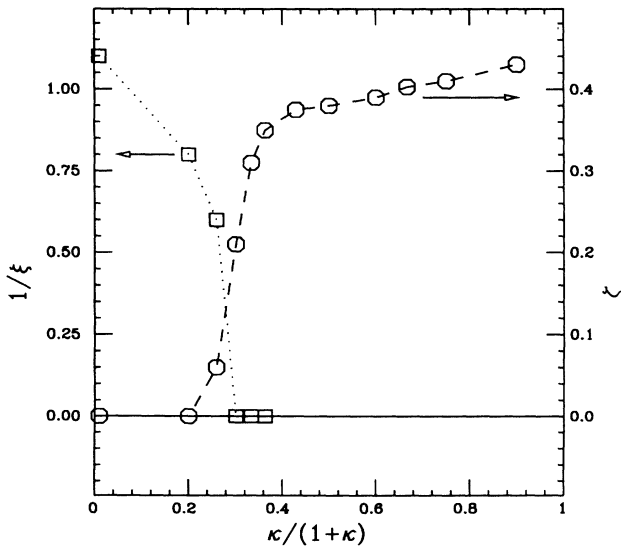

FIG. 9. Dependence of the extrapolated values of the parameters $1/\xi$ and ζ on the bending constant κ. Both quantities vanish as $\kappa \rightarrow \kappa_c$. The transition appears at $\kappa_c \approx 0.33$.

(connected) atoms, $0 < v' < 1$, and we have neglected numerical factors of order unity. For $\kappa \neq \kappa_c$, we can define a dimensionless correlation range $\Upsilon(\kappa)$ (measured in the units of nearest-neighbor distance) inside the surface, within which (5.3) holds and outside of which either of the cases in (5.2) obtains. Above T_c this length will be comparable to the correlation range of surface normals discussed in Sec. VII. We expect that $\Upsilon(\kappa)$ diverges at κ_c

$$\Upsilon(\kappa) \approx \begin{cases} \left[\dfrac{\kappa_c - \kappa}{\kappa_c} \right]^{-w_1} & \text{for } \kappa < \kappa_c \\[2ex] \left[\dfrac{\kappa - \kappa_c}{\kappa_c} \right]^{-w_2} & \text{for } \kappa > \kappa_c , \end{cases} \tag{5.4}$$

where the analogy with critical phenomena in ferromagnets suggests that $w_1 = w_2$.

Although our data do not permit accurate estimates of v', w_1, and w_2, we can relate these exponents to ξ and ζ via a simple scaling hypothesis: Far from the transition the radius of gyration should have the form

$$R_g \approx \begin{cases} a_1 \sqrt{\ln L} & \text{for } \kappa \ll \kappa_c \\ a_2 L & \text{for } \kappa \gg \kappa_c , \end{cases} \tag{5.5}$$

where a_1 and a_2 are microscopic lengths. Close to the transition we assume that the role of a_1 and a_2 will be played by (5.3) evaluated with $L = \Upsilon(\kappa)$

$$R_g(L) |_{L=\Upsilon(\kappa)} = a\Upsilon^{v'} . \tag{5.6}$$

The surface has broken up into crumpled fragments of size $a\Upsilon^{v'}$, each consisting of approximately $\Upsilon^2(\kappa)$ monomers, so that L should be replaced by L/Υ in Eq. (5.5), while a_1 and a_2 should be replaced by $a\Upsilon^{v'}$. Upon making these substitutions, we find that the radius of gyration near the transition behaves as in Eq. (5.2), with (neglecting logarithmic corrections)

$$\xi(\kappa) \approx a\Upsilon^{v'} \sim \left[\frac{\kappa_c - \kappa}{\kappa_c} \right]^{-v'w_1} \quad \text{for } \kappa < \kappa_c \tag{5.7a}$$

$$\zeta(\kappa) \approx a\Upsilon^{v'-1} \sim \left[\frac{\kappa - \kappa_c}{\kappa_c} \right]^{(1-v')w_2} \quad \text{for } \kappa > \kappa_c . \tag{5.7b}$$

Because $0 < v' < 1$ these scaling laws show that $\xi(\kappa)$ diverges as $\kappa \rightarrow \kappa_c^-$, while $\zeta(\kappa)$ tends to zero as $\kappa \rightarrow \kappa_c^+$, consistent with Fig. 9, although the limited accuracy of the data prevents extraction of the values of the exponents. (For a rough estimate of v', see Sec. VII.) One should keep in mind that, in fluid membranes, we would always expect that $\zeta = 0$, because the radius of gyration should have the crumpled form, $R_g \sim L^v$, with $v < 1$. In polymeric surfaces however, ζ in fact remains finite for large κ's, and vanishes at a finite value of κ. In this sense, $\zeta(\kappa)$ plays the role of an order parameter for the crumpling transition.

The finiteness of $\zeta(\kappa)$ at low temperature does not by itself prove that the surfaces are flat in the usual sense, since surfaces folded into, say, spherical or cylindrical shapes also have the property that $R_g \sim L$. Following Ref. 11, we expect the surface to be flat in a stricter

sense: its shape when embedded in 3D will have two dimensions significantly larger than the third one. A quantitative measure of such behavior in a random object is asphericity A defined as

$$A(\kappa,L) \equiv \left\langle \frac{R_1^2}{R_3^2} \right\rangle , \qquad (5.8)$$

where $\langle\ \rangle$ denotes configurational average, and R_1^2 and R_3^2 are, respectively, the minimal and the maximal principal moments of inertia, i.e., the minimal and maximal eigenvalues of the inertia tensor

$$T_{\alpha\beta} \equiv \frac{1}{N}\sum_i (\mathbf{r}_i)_\alpha (\mathbf{r}_i)_\beta - \frac{1}{N^2}\sum_{i,i'} (\mathbf{r}_i)_\alpha (\mathbf{r}_{i'})_\beta , \qquad (5.9)$$

where the Greek subscripts denote the Cartesian components of 3D coordinates of an atom. [The trace of this tensor coincides with R_g^2 defined in (5.1).] With definition (5.8), $A = 1$ for a sphere, and $A = 0$ for a flat surface. Measurements of A as a function of κ provide excellent evidence for the presence of the phase transition.

Figure 10 depicts $A(\kappa,L)$ for several values of L. For fixed L the asphericity is a monotonically decreasing function of κ. However, the increase in L affects differently the low- and high-temperature regions: for $\kappa > \kappa_c$, A decreases with increasing L, i.e., the surfaces become more flat, while for $\kappa < \kappa_c$ the surfaces become more spherical (A increases) with increasing L. In the limit $L \to \infty$, we expect that $A(\kappa,L)$ tends to zero for $\kappa > \kappa_c$. For $\kappa < \kappa_c$, $A(\kappa,L)$ should approach a universal, κ-independent, nonzero constant in this limit, in analogy with related results on the universality of polymer
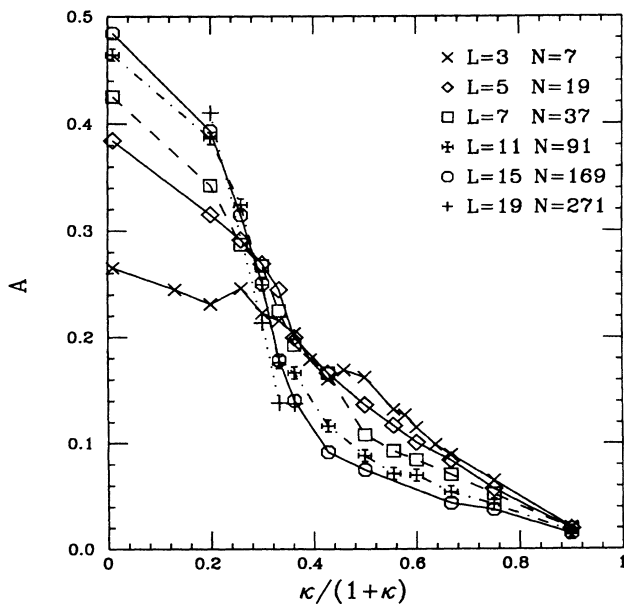
shapes.[17,18] We can estimate κ_c by following the L dependence of κ_1 and κ_2 defined, say, via $A(\kappa_1) \equiv 0.35$ and $A(\kappa_2) \equiv 0.15$, where κ_1 underestimates κ_c and is expected to approach κ_c as $L \to \infty$, while κ_2 overestimates κ_c and will decrease towards κ_c in that limit. Values of $\kappa_1/(1+\kappa_1)$ and $\kappa_2/(1+\kappa_2)$ have been obtained from the intersections of the interpolating lines in Fig. 10 with $A = 0.35$ and $A = 0.15$, respectively, and the results were depicted in Fig. 11 as a function of $1/L$. This result clearly indicates the presence of the critical point at $\kappa_c \approx 0.33$, which can be obtained by extrapolation to $1/L = 0$.

If the surface becomes flat in the large-κ regime, we may expect (for large L) to have $A \sim L^{-\rho}$, with $0 < \rho \le 2$, where small ρ corresponds to a very slow flattening out of the surface, while $\rho = 2$ corresponds to a surface with transverse fluctuations independent of its linear size L. Reference 11 provides two predictions of the asymptotic behavior of A: (a) According to discussion which follows Eq. (2.6) the mean-square transverse fluctuations $\langle f^2 \rangle \sim L$, and therefore $A \sim \langle f^2 \rangle /L^2 \sim 1/L$, i.e., $\rho = 1$; (b) crossover to this asymptotic behavior is delayed for larger values of κ. Our results permit a limited check of these predictions. Figure 12 depicts the L dependence of A for several values of κ, on a logarithmic scale. All graphs have a pronounced curvature, and it is impossible to extract their asymptotic behavior. A rough estimate of the asymptotic slope gives $\rho = 0.8\pm0.3$, which is consistent with $\rho = 1$ predicted in Ref. 11, and depicted as a straight line in Fig. 12. These results seem to be con-

FIG. 10. Asphericity A of the surface (ratio between the minimal and the maximal moments of inertia) as a function of κ for several values of L. The decrease of A with increasing κ becomes steeper for larger L.
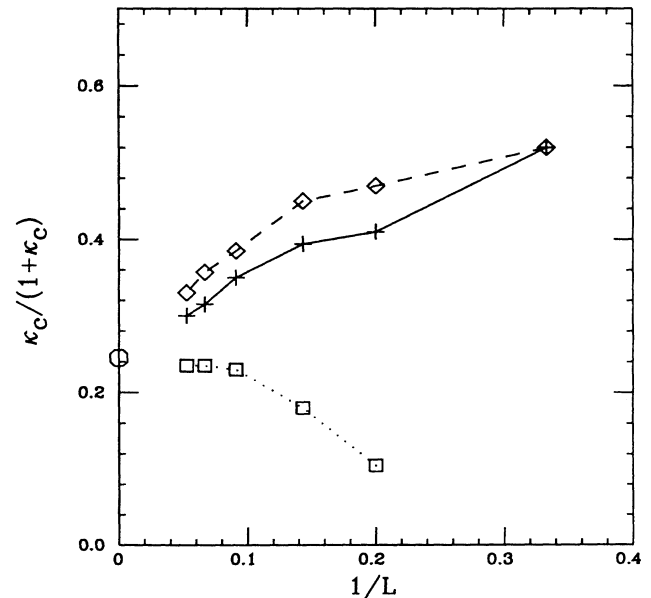

FIG. 11. Successive estimates of $\kappa_c/(1+\kappa_c)$ as a function of inverse surface size $1/L$, obtained from the point of maximum of the specific heat (crosses), from value of κ for which $A = 0.15$ (squares), and from value of κ for which $A = 0.35$ (diamonds). Circle on the vertical axis indicates the asymptotic value, corresponding to $\kappa_c = 0.33$.
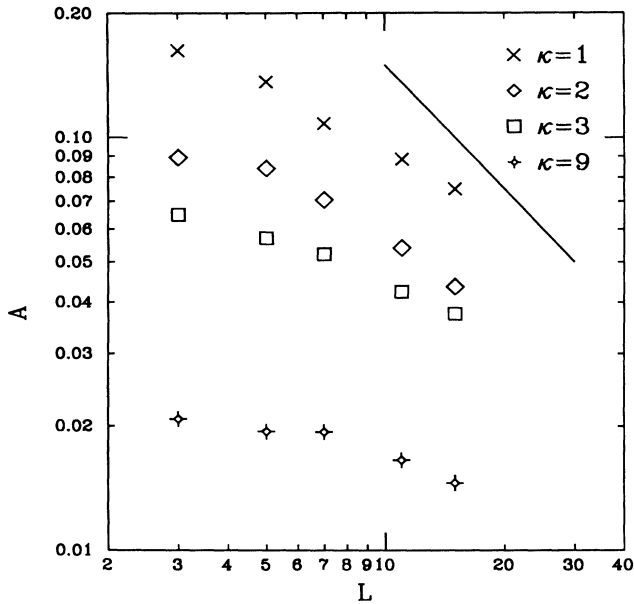
FIG. 12. Logarithmic plot of the asphericity A as a function of surface size L for several values of κ. Straight line indicates the slope of the dependence predicted in Ref. 11.

FIG. 13. Specific heat per atom C as a function of bending constant κ for several values of L. The peak in the specific heat becomes more pronounced for larger L.

sistent with the expectation that for large κ's we have a delayed crossover to the slope $\rho = 1$. On the basis of the available data we cannot, however, make any quantitative comparisons.

VI. SPECIFIC HEAT OF THE SURFACES

The presence of the phase transition is also clearly seen in the specific heat, which has been found from energy fluctuations in the surface. The only source of potential energy in our model is the bending energy of the surface. The specific heat per atom C can therefore be found from a simple expression

$$C = \frac{k_B \kappa^2}{N} \left[\left\langle \left[\sum_{\langle \alpha, \beta \rangle} \mathbf{n}_\alpha \cdot \mathbf{n}_\beta \right]^2 \right\rangle - \left\langle \sum_{\langle \alpha, \beta \rangle} \mathbf{n}_\alpha \cdot \mathbf{n}_\beta \right\rangle^2 \right] , \qquad (6.1)$$

where the summations are performed over all pairs of adjacent triangles, and the big $\langle \ \rangle$ denotes an average over the configurations. The dependence of C on κ is depicted in Fig. 13. (We suppress the trivial kinetic part $\frac{3}{2} k_B$ of the specific heat.) It has a well-pronounced peak, whose height increases with L.

For $\kappa = 0$, the fluctuations are purely entropic since the potential (2.2) allows only configurations with zero potential energy. Consequently, $C = 0$ at this point. For sufficiently large κ, one can neglect the coupling between the transverse fluctuations. The only contribution to the potential energy will come from the degree of freedom embodied in transverse oscillations. [The two additional (in-plane) degrees of freedom are entropic, and hence, do not contribute to specific heat.] Therefore, for large κ we expect to obtain $C = \frac{1}{2} k_B$, in accordance with
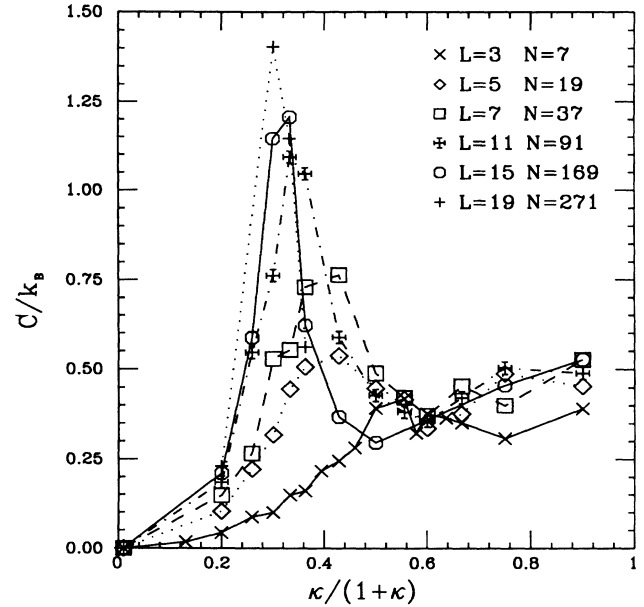
Dulong-Petit law. Indeed all the curves in Fig. 13 approach that limit for $\kappa \to \infty$. In the absence of a phase transition one might expect a smooth interpolation of C as κ changes from 0 to ∞. Figure 13, on the other hand, shows a pronounced peak, which sharpens for large L. The position of the peak appears to be drifting towards smaller κ's with increasing L. It does not tend to zero, however, but approaches a constant value. In Fig. 11 we plotted the positions of these peaks as function of $1/L$. (Since the values of κ, for which C has been measured are very sparse, we found the position of the peak by interpolating the data points by a smooth curve.) We observe that these results also converge to the same critical point which has been obtained from the measurements of κ_1 and κ_2.

Since our measurements have been performed for systems of quite limited size, we did not attempt to determine the critical index of the specific heat. Our data is, however, sufficient to practically exclude the possibility of a first-order phase transition. In the case of first-order phase transition the presence of latent heat or, equivalently, a δ-function singularity in the specific heat, will appear as a peak in a specific heat for small system sizes. Following the method of Ref. 19, one first assumes that the system undergoes a first-order transition, and concludes that the apparent height the specific heat peak C_m should increase linearly with N, with slope proportional to the squared jump in entropy. We do not see linear dependence of C_m on N (the graph curves), and the estimated latent heat decreases as we go to larger values of N. We estimate that the jump of the entropy at the transition point cannot exceed $0.08 k_B$, which supports our contention that we are dealing with a second-order phase transition.

VII. NORMAL-NORMAL CORRELATIONS

We have also explored the analogy between the surfaces and a 2D Heisenberg model by examining the correlations between the unit normals to the surface. Figure 14 shows the dependence of $\langle n(x) \cdot n(0) \rangle$ for an $L = 15$ on the distance x, which is measured in a Cartesian coordinate system (x_1, x_2) attached to the fluctuating surface, for variety of values of κ. For $\kappa > \kappa_c$ the normals are strongly positively correlated, suggesting a "ferromagnetic state." Finite-size effects due to the free boundary conditions obscure the expected approach of $\langle n(x) \cdot n(0) \rangle$ to a constant, however. Near the transition, finite-size effects are very important and we observed a pronounced L dependence of these correlation functions. At small κ, we expect the correlations to decay to zero. This effect is clearly seen for, say, $\kappa = 0.25$, where the correlations decay within few lattice spacings. The negative correlations observed for small x when $\kappa = 0.01$ and $\kappa = 0.25$ are due to folding of adjacent triangles in a highly crumpled phantom surface (see Fig. 4).

If the conjectured semicrumpled regime indeed exists we may expect power-law correlations between the normals at the length scales smaller than the correlation length, i.e., $\langle n(x) \cdot n(0) \rangle \sim x^{-\eta'}$. The exponent η' can be related to the exponent ν' via a simple argument:[20] we can calculate the algebraic projection $\mathcal{A}_p$ of the surface area of our membrane on a plane perpendicular to some arbitrary 3D unit vector p. We treat our surface as orientable, and therefore the projections may have both positive and negative signs, depending on whether the normal to the surface forms an angle smaller or larger than $\pi/2$ with p. Clearly,

$$\mathcal{A}_p = \int d\mathcal{A}_p = \int d^2x \, n_p(x) \, , \tag{7.1}$$

where $n_p \equiv p \cdot n$ is the projection of the normal on direction p. We now assume that the $\langle n_p(x) n_p(0) \rangle$ are correlated with the same power law as $\langle n(x) \cdot n(0) \rangle$.

Therefore, the configurational average of $\mathcal{A}_p^2$ satisfies

$$\langle \mathcal{A}_p^2 \rangle = \int d^2x \int d^2x' \langle n_p(x) n_p(x') \rangle$$

$$\approx L^2 \int d^2x \, \langle n_p(0) n_p(x) \rangle \sim L^2 \int d^2x \, \frac{1}{x^{\eta'}} \sim L^{4-\eta'} \, . \tag{7.2}$$

The above derivation assumes that the integrals are dominated by the upper (large-length-scale) cutoff, and, thus, is valid for $\eta' < 2$. If we now assume that $\langle \mathcal{A}_p^2 \rangle \approx R_g^4 \sim L^{4\nu'}$, we find that

$$\eta' = 4(1 - \nu') \, . \tag{7.3}$$

Our data is too crude to allow a direct reliable estimate of η'. However, we may use the value of ν' determined in Sec. VIII ($\nu' = 0.78 \pm 0.10$) and the relation (7.3) to obtain an estimate $\eta' \sim 0.8$.

VIII. EXCLUDED VOLUME EFFECTS

To make contact with real polymer surfaces, we must discuss effects of distant self-avoidance. In the flat phase, self-avoidance should be unimportant at long wavelengths. The behavior of asphericity displayed in Fig. 12, in particular, should be qualitatively unchanged. Its main effect is to augment the bending forces, thus delaying the transition to the crumpled state. Clearly, the critical temperature (i.e., κ_c^{-1}) found in this work is a *lower* bound on the critical temperature (i.e., an upper bound on κ_c) with self-avoidance. In the crumpled phase, on the other hand, self-avoidance plays a major role,[1] since it swells the surface and replaces the *logarithmic* dependence of R_g^2 on L, by a power law $R_g \sim L^\nu$ with $\nu \approx 0.8$. As in the semicrumpled case described in Sec. VII, the self-avoiding surfaces are expected to have power-law normal-normal correlations, with exponent $\eta = 4(1 - \nu) \approx 0.8$. Figure 15 shows these correlations,
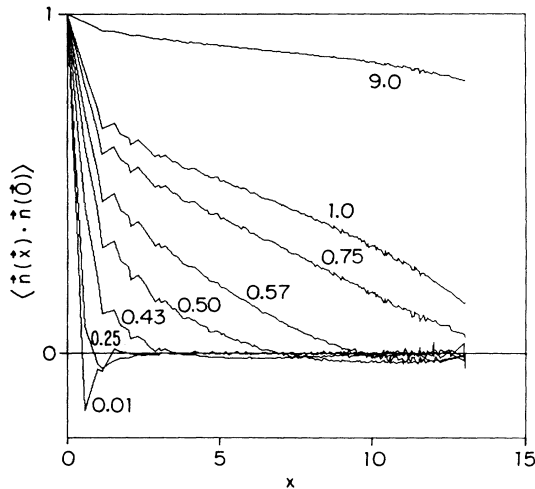

FIG. 14. Normal-normal correlation function in $L = 15$ hexagon as a function of the *internal* distance x (in lattice constants) for several values of κ (shown near the graphs).
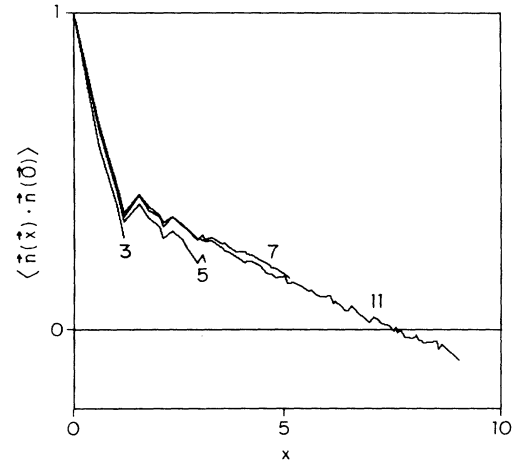

FIG. 15. Normal-normal correlation of *self-avoiding* surfaces without bending energy ($\kappa = 0$) for several values of L (indicated near the curves) as a function of the *internal* distance x (in lattice constants).

which have been measured on the surfaces with $\kappa=0$.[1] These correlations decay within few lattice constants, consistent with power-law correlations and a relatively large value of η. There is no indication of long-range order in the normal for $\kappa=0$, in contrast to the behavior expected in the large-κ flat phase discussed in this paper. Differences between the crumpled self-avoiding surface at $\kappa=0$ and the flat phase found for large κ (without self-avoidance, but in a regime where self-avoidance is irrelevant) suggest that *the transition will appear for $0<\kappa<\infty$ even in the presence of self-avoidance.*

The details of the transition are likely to be different, however. To show this we will use the results of our simulation at the transition point, i.e., in the semicrumpled regime and inquire about the relevance of a small excluded volume interaction. Figure 16 depicts the L dependence of R_g in the semicrumpled regime. The effective transition point was defined as a point of maximum in the specific heat. Value of R_g at that point has been found from the interpolating curves in Fig. 6. Since the points lie in steep region of the graphs in Fig. 6 (near the transition point the curves move from values of order $\ln L$ to values of order L^2) the uncertainties are quite large. Nevertheless, this procedure provides a rough estimate of ν'. From the slope of the graph in Fig. 16 we find $\nu'=0.78\pm0.10$. By examining the configurations created without excluded volume in the semicrumpled regime we find the number of overlapping atoms N_0 increases like $N_0\sim L^\omega$, with $\omega=3.6\pm0.3$. Thus in the presence of a very weak excluded volume interaction, the total excluded volume energy would increase with this power. The number of overlaps per unit volume n_0 scales like $n_0\sim L^\omega/R_g^3\sim L^y$, where
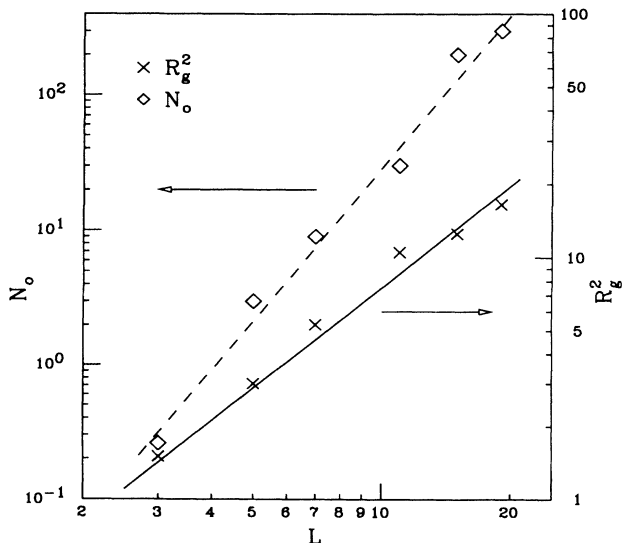

FIG. 16. Properties of semicrumpled surfaces as measured at the effective phase transition point (where the specific heat achieves its maximum): squared radius of gyration R_g^2 and the number of overlaps between atoms N_0, which measures the possible strength of the excluded volume effect, are shown as functions of surface size L on a logarithmic scale. Slopes of these graphs determine $2\nu'$ (R_g^2 graph), and $\omega(N_0$ graph).

$y=\omega-3\nu'$. According to our estimates y is positive, indicating that the density of self-intersections increases, as one goes to larger-length scales. This result suggests a new critical behavior at the transition for self-avoiding surfaces.

One can only speculate on the details of the transition in the presence of the excluded volume effect. In the presence of bending forces *and* self-avoidance we expect ν'_f of the new semicrumpled regime to be larger than ν, $0.8<\nu'\leq1$. The scaling relation (5.7b) for $\zeta(\kappa)$ will be unchanged, while (5.7a) must be replaced by

$$\xi(\kappa)\approx a\Upsilon^{\nu'-\nu}\sim\left|\frac{\kappa_c-\kappa}{\kappa_c}\right|^{-(\nu'-\nu)\omega_1}\quad\text{for }\kappa<\kappa_c\ .\qquad(8.1)$$

However, it may be difficult to distinguish numerically between the behavior on the length scales shorter and longer than the correlation length. It is even possible that there is no correlation length below κ_c. These possibilities indicate desirability of investigations of the surface including self-avoidance.

IX. DISCUSSION

Theoretical discussions of conventional linear polymers often exploit a remarkable analogy with second-order phase transitions:[5] as the molecular weight becomes large, a polymer behaves more and more like a magnet at its critical temperature. The radius of gyration grows with polymerization index like the correlation length near the Curie point. Flexible sheet polymers with low bending rigidity also display singular properties as they become large.[1] In this paper, we have explored via Monte Carlo simulations the suggestion[11] that there is *in addition* an unusual phase transition with increasing rigidity *within the polymer itself.* Although most of our computations are restricted to sheet polymers without self-avoidance, we have presented a strong evidence for an analogous transition in real self-avoiding membranes. Such a transition could be explored in the laboratory using low rigidity polymerized lipid bilayers[2,3] or systems similar to the crosslinked polymethyl methacrylate studied in Ref. 4.

In our simulations we found that the transition appears when $\bar\kappa/K_0\approx0.02$. In the presence of excluded volume interactions this value can be reduced even more. Because the elastic constants varied strongly with temperature in our simulation ($\lambda,\mu\propto k_BT$, for entropic reasons), the model studied here is strongly thermotropic. Polymerized lipid bilayers and monolayers should be less sensitive to temperature, however, because the bending constants and the in-plane elastic constants have similar molecular origin, $\bar\kappa/K_0$ should be a relatively weak function of T. One can get some idea about the possible range of these parameters by considering a *macroscopic* membrane. If it is made of isotropic material with Young modulus E and Poisson ratio σ, then[15] $\bar\kappa=h^3E/[24(1-\sigma^2)]$, where h is the thickness of the membrane. The coupling constant K_0 of such membrane will be $a^2hE/(1-\sigma^2)$. Thus the ratio $\bar\kappa/K_0=h^2/(24a^2)$, and for $a\sim h$ we may get ratios close to the critical values predicted in this simulation. We thus

expect that many microscopic systems will have parameter values close to the critical point, so that one can drive the system through the transition point by small variations of, for example, cosurfactant concentration, and the nature of the solvent.

Many interesting questions remain. What are the precise critical exponents without self-avoidance? Can one check or refine the prediction[11] that the renormalized rigidity increases with system size in low-temperature range? What is the nature of the finite-temperature transition which occurs when self-avoidance is taken into account? References 1 and 11 treat distinct model Hamiltonians which describe, respectively, the high- and low-temperature phases discussed in this paper. Both these have singular long-wavelength properties which are in-

teresting in their own right. Can one construct a tractable theoretical model which treats these phases as well as the transition between them in a unified way? It would be gratifying to learn the answers to some of these questions from further theoretical analysis and, more importantly, from real laboratory experiments.

ACKNOWLEDGMENTS

*Address since September 1987: School of Physics and Astronomy, Tel Aviv University, 69 978 Tel Aviv, Israel.

[1]Y. Kantor, M. Kardar, and D. R. Nelson, Phys. Rev. Lett. **57**, 791 (1986); Phys. Rev. A **35**, 3056 (1987).

[2]J. H. Fendler and P. Tundo, Acc. Chem. Res. **17**, 3 (1984). This reference discusses polymerization with bifunctional units. *Polyfunctional* polymerized units would be a better approximation to the tethered surfaces discussed here. For polymerization with crosslinking of a Langmuir monomolecular film, see N. Beredjick and W. J. Burlant, J. Polymer Sci. A **8**, 2807 (1970).

[3]J. Larche, J. Appel, G. Porte, P. Bassereau, and J. Marignan, Phys. Rev. Lett. **56**, 1700 (1986); C. R. Safinya, D. Roux, G. S. Smith, S. K. Sinha, P. Dimon, N. A. Clark, and A. M. Bellocq, *ibid.* **57**, 2718 (1986).

[4]A. Blumstein, R. Blumstein, and T. H. Vanderspurt, J. Colloid Interface Sci. **31**, 236 (1969).

[5]P.-G. de Gennes, *Scaling Concepts in Polymer Physics* (Cornell University Press, Ithaca, 1979).

[6]See, e.g., J. H. Weiner, *Statistical Mechanics of Elasticity* (Wiley, New York, 1979), Chap. 5.

[7]P.-G. de Gennes and C. Taupin, J. Phys. Chem. **86**, 2294 (1982).

[8]W. Helfrich, J. Phys. (Paris) **46**, 1263 (1985).

[9]L. Peliti and S. Leibler, Phys. Rev. Lett. **54**, 1690 (1985).

[10]A. M. Polyakov, Nucl. Phys. B **268**, 406 (1986).

[11]D. R. Nelson and L. Peliti, J. Phys. (Paris) **48**, 1085 (1987).

[12]Y. Kantor and D. R. Nelson, Phys. Rev. Lett. **58**, 2774 (1987).

[13]D. G. Gross, Phys. Lett. B **139**, 187 (1984).

[14]M. Kardar and D. R. Nelson, Phys. Rev. Lett. **58**, 1289 (1987); **58**, 2280 (E) (1987); J. A. Aronowitz and T. C. Lubensky, Europhys. Lett. (to be published); B. Duplantier, Phys. Rev. Lett. **58**, 2733 (1987).

[15]L. D. Landau and E. M. Lifshitz, *Theory of Elasticity* (Pergamon, New York, 1970).

[16]M. Parrinello and A. Rahman, J. Chem. Phys. **76**, 2662 (1982). Our definition is slightly different from this reference. The two definitions coincide for large systems.

[17]See, e.g., J. A. Aronovitz and D. R. Nelson, J. Phys. (Paris) **47**, 1445 (1986).

[18]M. Kardar and D. R. Nelson, and, independently B. Duplantier have shown (see Ref. 14) that certain critical indices depend on the *shape* of the boundary of two-dimensional manifold. This suggests that the limiting value of A may also depend on shape (a hexagon, in our simulations). We expect, however, universality as a function of κ in the crumpled phase, for a fixed shape.

[19]C. Dasgupta and B. I. Halperin, Phys. Rev. Lett. **47**, 1556 (1981).

[20]This argument was suggested to us by M. Kardar.